

## Core-level spectroscopy of hydrocarbons adsorbed on Si(100)-(2×1): A systematic comparison

A. Fink,<sup>1</sup> W. Widdra,<sup>1,\*</sup> W. Wurth,<sup>1,†</sup> C. Keller,<sup>1</sup> M. Stichler,<sup>1</sup> A. Achleitner,<sup>1</sup> G. Comelli,<sup>2</sup> S. Lizzit,<sup>3</sup>  
A. Baraldi,<sup>3</sup> and D. Menzel<sup>1</sup>

<sup>1</sup>Physik-Department E20, Technische Universität München, 85747 Garching, Germany

<sup>2</sup>TASC-INFM Laboratory, 34012 Basovizza, Trieste, Italy

and Dipartimento di Fisica, Università di Trieste, 34127, Trieste, Italy

<sup>3</sup>ELETTRA, Sincrotrone Trieste, 34012 Trieste, Italy

(Received 2 October 2000; revised manuscript received 16 February 2001; published 21 June 2001)

Adsorbate and substrate core-level binding energies for adsorption layers of six unsaturated hydrocarbons ( $C_2H_2$ ,  $C_2H_4$ ,  $C_3H_4$ ,  $C_4H_6$ ,  $C_6D_6$  ( $C_6H_6$ ), and 1,2- $C_2H_2Cl_2$ ) on the Si(100)-(2×1) surface have been determined by high-resolution x-ray photoemission spectroscopy; results for the clean and the (2×1)-H covered surface have been obtained for comparison. Remarkable differences in the Si 2*p* and C 1*s* surface core-level shifts for the various adsorbates are found, which range from 327 to −169 meV and from 1220 to −260 meV, respectively. Both initial- and final-state effects are necessary to explain the strong but unsystematic variations of the observed shifts. Additionally, from a comparison of the C 1*s* intensities the absolute saturation coverages are determined to be 0.87, 0.84, 1.15, 0.79, 0.36, and 0.44 molecules per unit cell of the clean surface for  $C_2H_2$ ,  $C_2H_4$ ,  $C_3H_4$ ,  $C_4H_6$ ,  $C_6D_6$ , and 1,2- $C_2H_2Cl_2$ , respectively.

DOI: 10.1103/PhysRevB.64.045308

PACS number(s): 73.20.-r, 73.61.Cw, 79.60.-i

### I. INTRODUCTION

Due to the evolution of semiconductor fabrication and the industrial needs for high-speed and high-temperature semiconductor devices, the material SiC has come into the focus of research.<sup>1,2</sup> As a substrate for SiC growth by chemical vapor deposition, the flat and stepped Si(100) surface is of great technological importance. Often the adsorption and decomposition of unsaturated hydrocarbon molecules are used as the initial stages of carbonization of the Si(100) surface.<sup>3,4</sup> For the carbonization process unsaturated hydrocarbons are favored because of their higher reactivity at lower temperatures compared to saturated molecules; this avoids dopant redistribution in the silicon substrate.<sup>5</sup> Therefore adsorption, thermal behavior, decomposition, and the electronic structure of unsaturated small molecules on Si(100) surfaces have been investigated as model systems. The additional interest in well-defined interfaces between Si(100) and organic material arises from their role in technological areas such as molecular electronics and sensors.

Although many aspects of the adsorption of small hydrocarbon molecules on Si(100) have been quite extensively investigated, there is a lack of detailed information on the core-level binding energies,<sup>6–8</sup> which would supply information on adsorbate-induced charge redistribution in the ground-state and screening changes. While the bare Si(100) surface has been well investigated in the past with high-resolution x-ray photoemission spectroscopy (XPS),<sup>9–12</sup> leading to deep insight into the complexity of surface core-level shifts (SCLS's), charge transfer, and screening, the effects of hydrocarbon adsorbates on Si(100) on these aspects have been little investigated so far. We have therefore investigated six different hydrocarbon adsorbates,  $C_2H_2$ ,  $C_2H_4$ ,  $C_3H_4$ ,  $C_4H_6$ ,  $C_6D_6$ , and 1,2- $C_2H_2Cl_2$ , on a Si(100)-(2×1) surface under otherwise identical conditions. Since these adsorbates are interesting candidates for structural determination using photoelectron diffraction or holography,<sup>13,14</sup> we used single-domain Si(100) surfaces with an intentional mis-

cut of 5° toward the [011] direction. Here we present a systematic study of the surface Si 2*p* and the C 1*s* core-level shifts by high-resolution XPS using synchrotron radiation.

### II. EXPERIMENT

The experiments were performed at the SuperESCA beamline at ELETTRA, Trieste, Italy. The ultrahigh-vacuum chamber, with a base pressure of  $5 \times 10^{-11}$  mbar, is equipped with an argon-ion sputter gun, a quadrupole mass spectrometer, a rear-view low-energy electron-diffraction (LEED) system, and a hemispherical electron analyzer (VSW Class150) with 150 mm mean radius and a 16-channel detector. The Si sample was mounted on a low-temperature manipulator which has four degrees of freedom, and allows a fast cooldown to 80 K using liquid nitrogen as the coolant. The Si(100) sample was P doped (resistivity in the range of 8–12  $\Omega$  cm, Virginia Semiconductors) with an intentional miscut of  $5.0^\circ \pm 0.5^\circ$  in the [011] direction. It was mounted by a multilayer bonding technique via thin platinum and silver interlayers on a tantalum plate.<sup>15</sup> The sample was heated by electron bombardment, and the temperature was measured with a chromel-alumel thermocouple spot welded to the back of the tantalum plate. The surface was cleaned by repeated cycles of argon-ion sputtering, both at low temperatures and at 800 K, with subsequent annealing to 1150 K and slow cooling (−2 K/s) to 400 K. XPS showed no contaminations after several cycles, and the LEED pattern revealed sharp spots indicating a well-ordered single-domain 2×1 surface. After each experiment the same cleaning procedure was repeated. The hydrocarbon molecules were adsorbed at low temperatures (80–100 K) followed by sample annealing to 150–200 K in order to desorb multilayers. All experiments presented here were performed at saturation coverage of the hydrocarbon adsorbates. During the XPS measurements no changes in the spectra were observed, which indicated that there was no measurable light or secondary-

electron-induced decomposition or desorption of the chemisorbed hydrocarbon molecules.

All photoemission experiments were carried out with a fixed angle of  $45^\circ$  between the hemispherical analyzer and the incident light beam.<sup>16</sup> The photoelectrons were detected at emission angles of  $0^\circ$ ,  $70^\circ$ , and  $80^\circ$  with respect to the surface normal. The light polarization and the plane defined by light incidence and electron emission were aligned along the Si-Si dimer rows. Si  $2p$  and C  $1s$  spectra were measured with photon energies of 182 and 391 eV, respectively. Using the Fermi edge of the metal support, an upper limit of 120 meV for the combined experimental resolution can be given.<sup>42</sup>

For all spectra, the Si  $2p$  core level of the Si bulk component was used as an internal energy standard such that the Si  $2p_{3/2}$  bulk component was set to 99.20 eV. For the C  $1s$  spectra the Si  $2p$  region was measured directly after the C  $1s$  region without changing the photon energy or experimental geometry. Using this internal reference energy we can rule out different band bendings for the various adsorbate systems as being the origin of the core-level shifts observed here (with an upper limit of 20 meV), in contrast to earlier suggestions.<sup>17</sup>

### III. RESULTS AND DISCUSSION

#### A. C $1s$ core levels

X-ray photoemission spectra of the C  $1s$  core level for six hydrocarbon adsorbates ( $C_2H_2$ ,  $C_2H_4$ ,  $C_3H_4$ ,  $C_4H_6$ ,  $C_6H_6$ , and 1,2- $C_2H_2Cl_2$ ) on the Si(100)-(2 $\times$ 1) surface at saturation coverage are shown in Fig. 1 for a photon energy of 391 eV and an electron emission angle of  $70^\circ$  with respect to the surface normal. Figure 1 shows that the C  $1s$  spectra of  $C_2H_2$ ,  $C_2H_4$ ,  $C_4H_6$ , and  $C_6H_6$  exhibit only one peak each, while in the spectra of  $C_3H_4$  and 1,2- $C_2H_2Cl_2$  two peaks are discernible. It is also obvious that the energy positions of the C  $1s$  core levels of the different hydrocarbons vary significantly. Since the intensities of the C  $1s$  core level peaks are normalized to the background on the low-binding-energy side, the peak areas can be directly compared with each other. Symmetric Voigt functions are not applicable to fit the C  $1s$  spectra because of the clear asymmetry of the peaks. Even for spectra which show only one peak, e.g., the  $C_2H_4$  spectrum, more than one symmetric Voigt peak would be necessary to fit the data, and there is no evidence of more than one component in any of the single-peak spectra, e.g., by a shoulder in the spectra. An attempt to fit the asymmetric peaks with two Voigt peaks failed, which can be taken as additional evidence that asymmetric peak shapes are the best choice.

In the case of  $C_2H_2$  only one asymmetric peak can be derived from our data, at an energy position of 283.98 eV and with a full width at half maximum (FWHM) of 0.75 eV, in contrast to the two symmetric peaks presented in Refs. 6 and 18. However this is no contradiction, because in this earlier work acetylene was adsorbed at a temperature of 1093 K, at which acetylene decomposes and forms SiC on the surface. The resulting two C  $1s$  peaks have been interpreted as carbon bound to carbon and carbon bound to silicon.

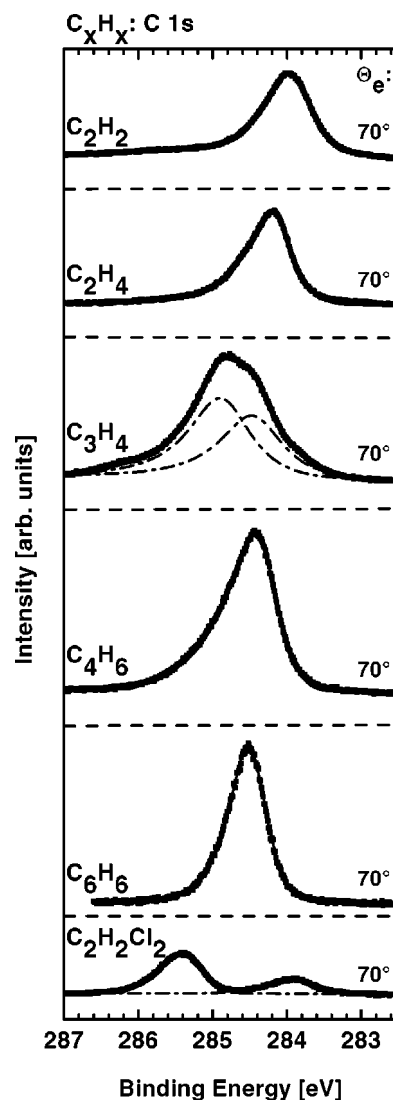


FIG. 1. C  $1s$  core-level spectra for adsorbate layers of  $C_2H_2$ ,  $C_2H_4$ ,  $C_3H_4$ ,  $C_4H_6$ ,  $C_6H_6$ , and 1,2- $C_2H_2Cl_2$  on Si(100)-(2 $\times$ 1). The spectra were taken at 391 eV photon energy, and an emission angle of  $70^\circ$  with respect to the surface normal.

Similarly, after annealing the saturated acetylene layer to 1000 K we find two peaks in the C  $1s$  spectra separated approximately 1.3 eV from each other. In Ref. 7 a main peak was also observed at 283.9 eV, similar to ours (283.98 eV). However, that work found a shoulder at 284.7 eV,<sup>43</sup> corresponding to 25% of the total peak area which is absent in our spectra.

For  $C_2H_4$  a single peak is also observed, located at 284.21 eV, with a FWHM of 0.70 eV. A clearly asymmetric peak shape tailing toward the high-energy side can be seen in Fig. 1, which may be due to vibrational structure as speculated in Ref. 8. Similarly, an asymmetric main peak was observed in Ref. 8, with a small additional peak approximately 1.1 eV below the main peak which is absent in our spectra. In Ref. 8 this additional feature was attributed to a  $C_2H_4$  decomposition product. However, as shown, e.g., in Refs. 19 and 20, in the absence of coadsorbates no significant decomposition of

$C_2H_4$  is found which could account for the additional feature. Only when the sample was not well cleaned before ethylene adsorption and carbon was still present on the surface, we did observe a small, unspecific shoulder (about 1.2–1.4 eV below the main peak) on the low-energy side of the  $C_2H_4$  C 1s spectrum. In Ref. 7 a single C 1s peak for  $C_2H_4/Si(100)$  was also observed at approximately 400 meV lower binding energy than here, with an increased FWHM of 0.9 eV (0.7 eV in our study).

Similarly to  $C_2H_2$  and  $C_2H_4$ , only one C 1s peak is observed for adsorbed  $C_4H_6$  (FWHM of 0.83 eV). Although the width is wider than seen for  $C_2H_2$  or  $C_2H_4$  we cannot separate it into different components. The C 1s core levels of the four carbon atoms appear to be energetically roughly equivalent, despite their unequal chemical surroundings due to the fact that two carbon atoms form bonds to the silicon substrate and two do not (see Ref. 21).

As in the case of  $C_4H_6$  the C 1s core levels of the different carbon atoms of adsorbed benzene ( $sp^3$  and  $sp^2$  hybridized) are energetically indistinguishable within the peak width of the experiment ( $\Delta E < 120$  meV).  $C_6H_6$  again shows a slightly asymmetric peak. In order to investigate the nature of the peak asymmetry, deuterated benzene molecules were used in additional experiments. If the asymmetry would stem from unresolved vibrational fine structure, it should differ considerably for  $C_6H_6$  and  $C_6D_6$  (C-H stretching vibrations: 375 and 265 meV for C-H and C-D, respectively). However for  $C_6H_6$  and  $C_6D_6$  the same asymmetry was found (not shown). This indicates that the asymmetry of the C 1s peak is not caused by unresolved C-H stretching vibrations. Only for 1,2- $C_2H_2Cl_2$  were two well-separated peaks in the C 1s spectra observed. The C 1s spectrum of  $C_3H_4$  exhibits a broad structure with a large FWHM of 0.97 eV, which can be separated into two peaks at 284.49 and 284.90 eV, respectively.

In the following the saturation coverages of the different hydrocarbon adsorbates on the Si(100) surface will be discussed. To gain an absolute carbon coverage scale we use the property of  $C_2H_2$  that it decomposes at elevated temperatures, liberating approximately all (see below) of its hydrogen molecularly into the gas phase.<sup>22–25</sup> The amount of hydrogen, as determined in quantitative thermal desorption experiments (shown elsewhere<sup>26</sup>), can be compared with the signal from the well-ordered Si(100)-(2×1)-H monohydride phase which corresponds to two H atoms per 2×1 unit cell (one H atom per dimer atom). Additionally there exists a minor reaction path which leads to molecular  $C_2H_2$  desorption. From the changes of the C 1s intensity upon annealing, an estimate of 5% for molecular desorption can be extracted from our data, as also found earlier by electron-induced Auger electron spectroscopy.<sup>22</sup> Based on these comparisons the absolute  $C_2H_2$  coverage is determined to 0.87 molecules per 2×1 unit cell.

On this basis the saturation coverages of the other hydrocarbons can be directly expressed in units of molecules per 2×1 unit cell of the Si(100) substrate. Taking the number of carbon atoms in the different hydrocarbon molecules into account, the experimentally determined saturation coverages

are 0.87, 0.84, 1.15, 0.79, 0.36, and 0.44 molecules per 2×1 unit cell for  $C_2H_2$ ,  $C_2H_4$ ,  $C_3H_4$ ,  $C_4H_6$ ,  $C_6H_6$ , and 1,2- $C_2H_2Cl_2$ , respectively. The absolute accuracy is about 10% due to the calibration, whereas the relative accuracy is better. An additional systematic error which is in principle always present in any quantitative XPS study from a crystalline sample (at a fixed solid angle) is related to photoelectron diffraction. Strong diffraction effects are expected for photoelectron kinetic energies in the range up to 500 eV, and therefore might be important here. For  $C_2H_4$  on Si(100) it has been shown that the C 1s modulation function reaches values up to 50% at normal emission, and a kinetic energy of 160 eV.<sup>13</sup> However, at about 100-eV kinetic energy, as used in this study, lower values have been found.<sup>13,27</sup> Furthermore, since the diffraction is dominated by backscattering (180° scattering), with some additional forward focusing for the case of an additional atom in the exit direction, the modulation function is highest for normal emission and decays quickly with the polar angle to a value below 10% for systems like  $C_2H_4$  on Si(100).<sup>13</sup> Since in all our cases the carbon atoms are located well above the topmost Si layer, we expect the backscattering from Si to be peaked to small polar emission angles. Most of the carbon atoms of the adsorbates investigated here are located close to or in the plane which contains both Si-Si dimer atoms. Since we used a grazing photoemission angle of 70° in a plane *perpendicular* to this plane (along the dimer row azimuthal direction) the experimental geometry is outside of any backward or forward scattering condition. Therefore we expect the diffraction effects to be below 20% (with a possible exception of  $C_2H_2Cl_2$  due to the heavier chlorine and its unknown location). The important implications of the observed saturation coverages on the adsorption models will be discussed elsewhere, while we focus on SCLS's here.

### B. Si 2p core levels

Si 2p core-level spectra for the same hydrocarbon adsorbates on Si(100) as described above have been measured under identical conditions. Only the photon energy was changed to 182 eV in order to enhance the surface sensitivity of the outgoing photoelectrons. In the following, data measured at polar emission angles of 0° (more bulk-sensitive) and 70°/80° (surface sensitive) will be discussed.

The bulk- and surface-sensitive measurements of the Si 2p core levels for the clean Si(100)-(2×1) surface are presented in the upper two spectra of Fig. 2. Following the notation of Landemark *et al.*<sup>9</sup> the components of the clean Si(100)-(2×1) surface are denoted by B, S, SS, S', and C for bulk, dimer up, dimer down, second layer, and third layer atoms, respectively. The spectra compare well with the results of the pioneering high-resolution study by Landemark *et al.*<sup>9</sup> Taking the fitting parameters of Landemark *et al.* and allowing larger Gaussian widths to account for the lower experimental resolution due to the higher photon energy used in our experiment, we can model our data very well. Since we used a 5° vicinal surface, this result indicates that an additional step-related component is not discernible from the data.

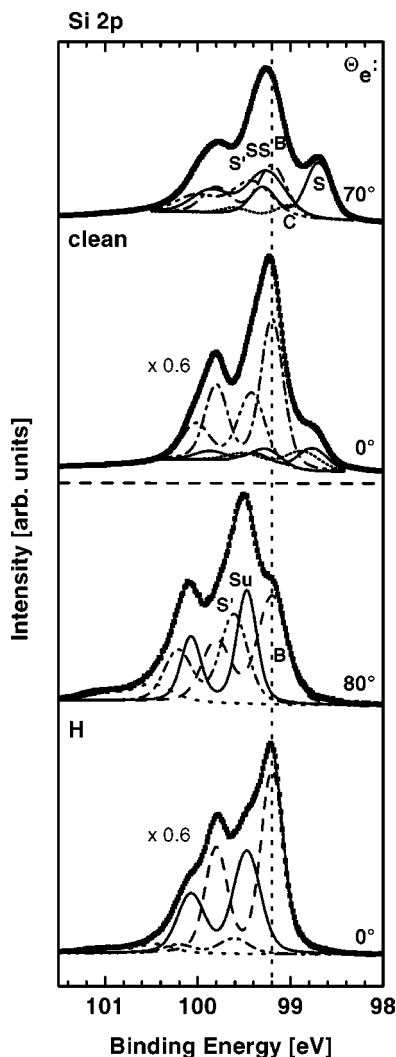


FIG. 2. Si  $2p$  core-level spectra for the clean  $5^\circ$  vicinal Si(100)-(2 $\times$ 1) surface and the well-ordered Si(100)-(2 $\times$ 1)-H monohydride layer at 182-eV photon energy and emission angles of  $70^\circ$  or  $80^\circ$ , and  $0^\circ$ . The bulk position of the Si  $2p_{3/2}$  core level is marked with a dotted line. A fit into different components of spin-orbit-split Si  $2p$  doublets is indicated by lines (see text).

Si  $2p$  spectra of the saturated monohydride layer are shown in the lower part of Fig. 2. A bulk component ( $B$ ), a surface component ( $Su$ ), and a second layer component ( $S'$ ) can be distinguished in the spectra. Note that a component  $S'$  (second-layer Si atoms) must be added in order to maintain constant peak positions in the bulk- and surface-sensitive spectra. A hydrogen-induced SCLS of +273 meV is derived which compares well with the shift of +260 meV reported earlier.<sup>28</sup> The spectra for Si(100)-(2 $\times$ 1)-H in Fig. 2 demonstrate nicely how the different intensities of the bulk and surface components for normal and grazing photoemission help to determine the SCLS's. This will be important for the other adsorbate systems.

The Si  $2p$  spectra for the different hydrocarbon adsorbates at saturation coverage are shown in Figs. 3 and 4, together with a deconvolution into different doublets. For this purpose the Si  $2p$  spectra have been fitted by three symmet-

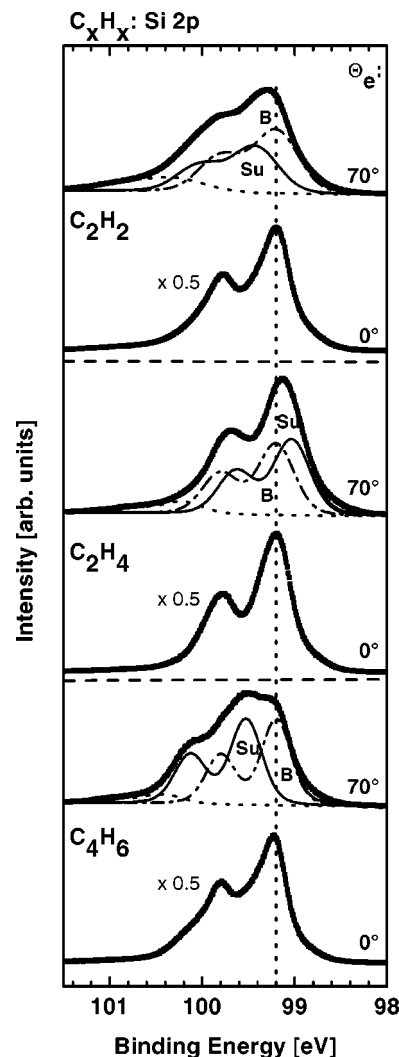


FIG. 3. Si  $2p$  core-level spectra for saturation coverages of  $C_2H_2$ ,  $C_2H_4$ , and  $C_4H_6$  on Si(100)-(2 $\times$ 1) measured at 182 eV photon energy and emission angles of  $70^\circ$  and  $0^\circ$ . Fits into different components of spin-orbit-split doublets are indicated by lines.

ric Voigt doublets (for the surface component, the bulk component, and a weak third component) with equal widths within each doublet. We have used the *same* constraints for fitting *all* Si  $2p$  XPS data of *all* hydrocarbon adsorbates. The spin-orbit splitting of the Si  $2p$  doublets was iteratively determined in order to match best *all* Si  $2p$  bulk and surface-sensitive spectra to  $602 \pm 5$  meV, which is compatible with Ref. 9. In the same way a Lorentzian width of 85 meV and a branching ratio of Si  $2p_{3/2}$ :Si  $2p_{1/2}$  = 1.75:1 were derived. The Gaussian width was fitted for each single peak separately, but constantly within a single doublet. A steplike function was used to model the secondary background. Alternative fits using two asymmetric Voigt doublets or three asymmetric Voigt doublets have been tested, but did not result in better fits. Some deficiencies of the fits in the tails of the peaks were found which show that the used fitting profiles cannot describe the data in *all* details, and that a slight reduction in the Lorentzian width could be compensated for by an increase of the Gaussian width and vice versa.

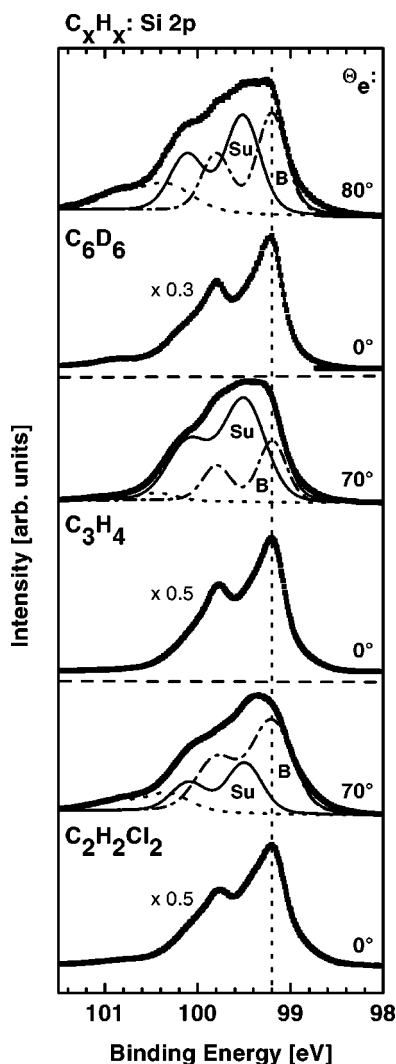


FIG. 4. Si  $2p$  core-level spectra for saturation coverage of  $C_6D_6$ ,  $C_3H_4$ , and 1,2- $C_2H_2Cl_2$  on Si(100)-(2 $\times$ 1) measured at 182 eV photon energy and emission angles of 70° and 0°.

For the saturated  $C_2H_2$  layer the comparison of the spectra for different emission angles which are presented in Fig. 3 allows one to identify a bulk component and a surface component. Both components seem to be rather broad. Note that two different surface components close to each other cannot be ruled out, but would explain the increased width. We find a positive SCLS of +227 meV which is attributed to the first-layer dimer atoms. The observation of a positive shift is in disagreement with a recent interpretation of Si  $2p$  spectra for the same system.<sup>17</sup> Although their spectra are rather similar to ours, Xu *et al.* presented a different interpretation with a surface component at  $-239$  meV.<sup>17</sup> This difference is most likely related to their assumption of a shift of the core-level spectra due to band bending (about 200 meV). This shift is the major difference in the otherwise rather similar spectra. However, on the basis of the direct comparison of spectra at normal and grazing emission shown in Fig. 3, we can rule out any significant component with a negative core-level shift. This example shows clearly that in the absence of distinct signatures in the raw data, additional

information (here the rigid position of the bulk component in the normal emission spectrum) is required to safely distinguish several components.

For the saturated  $C_2H_4$  layer the Si  $2p$  raw spectra, as presented in Fig. 3, reveal a broad doublet. However, from the comparison of surface- versus bulk-sensitive spectra, the existence of two doublets follows. The second component partially fills the valley between the  $2p_{1/2}$  and  $2p_{3/2}$  bulk peaks in the surface-sensitive spectrum. The surface core level is shifted by  $-169$  meV to lower binding energies. Note that in a previous work on  $C_2H_4/Si(100)$ <sup>8</sup> no resolvable adsorbate-induced core-level shift was found in their normal-emission spectra. Again the comparison of normal and grazing emission spectra enables the determination of the SCLS.

The surface-sensitive Si  $2p$  spectrum for  $C_4H_6$ , as presented in Fig. 3, resolves two doublets which can be attributed to the bulk and a  $+327$  meV shifted surface component. The poor agreement of the fit with the raw data on the low-binding-energy side at approximately 98.8 eV may be due to intensity from unreacted Si-Si dimers because the saturation coverage is lower than unity.

The Si  $2p$  surface-sensitive spectrum for the benzene-saturated Si(100) surface shows a broad, rather featureless structure (Fig. 4). With additional information from the bulk-sensitive data, the main features in the spectra can be described by two doublets with a surface component shifted by  $+315$  meV to higher binding energies. It is known that benzene adsorbs on every second Si-Si dimer by the formation of two Si-C  $\sigma$  bonds.<sup>29</sup> However, not much is known about the structures of the Si-Si dimers in between. Most likely they will buckle as on the clean surface which would lead to charge transfer and correspondingly to two shifted surface components similar to the clean surface (*S* and *SS* in Fig. 2). One of them (dimer up atom *S*) might explain the intensity at 98.8 eV (98.7 eV on the clean surface); the second is expected close to the bulk position, and would contribute to the bulk doublet here. The origin of the third component around 100.5 eV will be discussed below.

For the saturated  $C_3H_4$  layer (Fig. 4) we find broad Si  $2p$  spectra in the surface-sensitive geometry which can be deconvoluted into a dominating surface component (*Su*) and a bulk component. The rather broad surface component might be the result of several surface components which are not resolved here, but are expected based on the details of the C  $1s$  spectrum.

The chlorinated ethylene 1,2- $C_2H_2Cl_2$  possesses a broad surface-sensitive Si  $2p$  spectrum, as presented in Fig. 4. The SCLS of  $+296$  meV is remarkably different from the unchlorinated ethylene  $C_2H_4$  (Fig. 3). The strong intensity of the bulk component in the grazing-emission spectrum could indicate a second surface component close to the bulk component.

In some of the Si  $2p$  spectra for the individual adsorbate systems intensity at higher binding energies is visible which we modeled by a weak third doublet (at 1.01–1.25 eV for the various systems). Its intensity relative to the bulk component increases with increasing surface sensitivity of the measurement. Thus it is related to the silicon surface. A second ad-

sorbate species, which could be related to the adsorption at the  $D_B$  steps of the vicinal surface, is unlikely due to the relatively large SCLS's. Moreover the intensity of this component relative to the surface component varies by a factor of 7 within the different hydrocarbon systems, while the number of adsorption sites at the steps remains constant. We can also rule out a surface contamination, as, e.g., dissociatively adsorbed water which causes a Si  $2p$  SCLS of 1.1 eV,<sup>30</sup> since it is not found on the most reactive, clean surface. Furthermore the SCLS varies for the different hydrocarbon systems, which would be unlikely for a common contamination. Also the intensities vary significantly for the different hydrocarbon adsorbates, even exceeding the number of available adsorption sites in the case of  $C_2H_2$ . Therefore, we attribute this weak component to a shake-up satellite of the hydrocarbon modified surface.

### C. Relative core-level shifts

For an attempt at understanding the sequence of the core-level shifts, a few points should be kept in mind. Conceptually core-level shifts contain initial-state effects (adsorbate-induced charge redistribution in the ground state) and final-state effects (change of screening of the core hole).<sup>31</sup> An initial-state effect can be caused by the chemical environment of the particular atom from which the detected photoelectron originates. Different chemical environments can be given by different numbers of neighboring atoms, or the chemical environment can be altered if neighboring atoms are substituted by species with different electronegativity, e.g., in the case of  $C_2H_4$  versus 1,2- $C_2H_2Cl_2$ . In general chemical shifts can lead to higher or lower binding energies of the observed photoelectron. Final-state effects contributing to the observed core-level shifts stem from changes in the relaxation of the core-ionized system due to differences in the effective screening of the core hole. Screening can stem from a polarization of the surroundings by core hole creation or by dynamic charge transfer from a neighboring atom. Since an initial-state change of the ground-state charge distribution will also change the possible relaxation processes, there is a coupling between both contributions whose separation is only possible in model calculations. Nevertheless we attempt a qualitative discussion in these terms.

We will start with a comparison of the C  $1s$  core-level energies for the adsorbed molecules with those of the corresponding hydrocarbon molecule in the gas phase. The C  $1s$  ionization potentials (binding energies referenced to the vacuum level) for  $C_2H_2$ ,  $C_2H_4$ ,  $C_4H_6$ ,  $C_3H_4$  ( $sp$ ),  $C_3H_4$  ( $sp^3$ ),  $C_6H_6$ ,  $CH_4$ ,  $C_2H_6$ , and  $C_3H_8$  in the gas phase have been determined in different studies to 291.2,<sup>32</sup> 290.8,<sup>33</sup> 290.4,<sup>34</sup> 290.7,<sup>35</sup> 291.3,<sup>35</sup> 290.4,<sup>32</sup> 290.83,<sup>36</sup> 290.71,<sup>36</sup> and 290.57 eV,<sup>36</sup> respectively. The ionization potentials (shifted by  $-6.59$  eV for convenient line-up and ease of comparison) are compared with the C  $1s$  core levels of the adsorbate systems in Fig. 5. Our estimated experimental error for the adsorbate C  $1s$  binding energies is approximately  $\pm 20$  meV, while the error for the gas phase energies varies from 20 meV for, e.g.,  $CH_4$ ,<sup>36</sup> to 700 meV for  $C_6H_6$ .<sup>32</sup> Comparing the gas-phase ionization potentials of  $C_2H_6$ ,  $C_2H_4$ , and

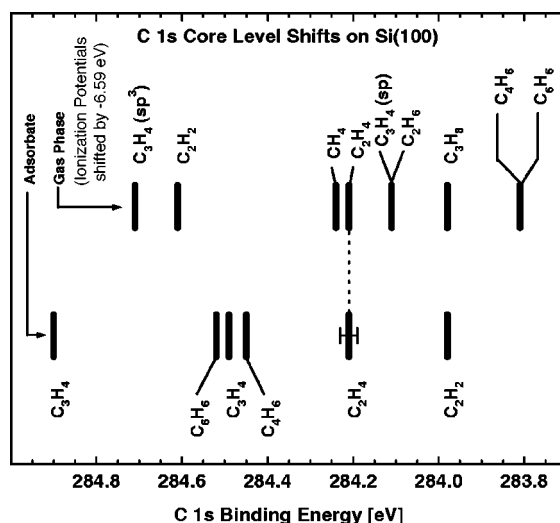


FIG. 5. C  $1s$  binding energies of various hydrocarbon molecules in the gas phase and adsorbed on Si(100)-(2 $\times$ 1). The gas-phase values are taken from Refs. 32–36 and 41 and have been shifted by  $-6.59$  eV for convenient comparison.

$C_2H_2$  one finds an up shift of the binding energy with the decrease of the hybridization from  $sp^3$  via  $sp^2$  to  $sp$ . Comparing the saturated alkanes,  $CH_4$ ,  $C_2H_6$ , and  $C_3H_8$ , a down shift with the alkane length is observed which is most likely due to increased screening.<sup>36</sup> A combination of these two effects may be responsible for the C  $1s$  energies of  $C_6H_6$  and  $C_4H_6$ . However, such simple rules can also fail as seen for the different C atoms of  $C_3H_4$ , which are  $sp$  and  $sp^3$  hybridized. Here the  $sp$ -hybridized atom has the lower binding energy. For the adsorbed molecules no analogous rules can be found; e.g., for  $C_2H_2$  and  $C_2H_4$ , the observed sequence is reversed compared to the gas phase. A direct comparison of the C  $1s$  binding energies of the hydrocarbon molecules in the gas phase and upon adsorption as shown in Fig. 5, does not show any systematic correlation between the gas phase and adsorbed phase. The chemical and the relaxation shifts for the C  $1s$  level are clearly changed differently upon chemisorption on the Si surface, although adsorption might be quite similar (di- $\sigma$  bonding) for all adsorbates.

All core-level shift data are summarized in Table I, and Fig. 6 graphically shows the various Si  $2p$  SCLS's. The SCLS's for the clean Si(100) surface,  $-488$  and  $+62$  meV, are directly related to the charge redistribution from the dimer-down to the dimer-up atom of the asymmetric Si-Si dimer.<sup>9</sup> Calculations by Pehlke and Scheffler have shown that relaxation effects play a crucial role for the understanding of the relative SCLS's, in addition to the static initial-state shifts.<sup>11</sup> All adsorbates discussed here lift the up-down splitting of the clean surface and lead to symmetric dimers. For part of the systems this is known directly; for the other parts it is suggested by spectroscopic information including the SCLS values reported here. If one wants to consider the influence of the adsorbate on the SCLS, then the point of reference should really be the hypothetical clean surface with symmetric dimers. Taking simply the mean value of the "up" and "down" values of the clean surface as references

TABLE I. Positions of the C  $1s$  and Si  $2p_{3/2}$  surface core levels for the clean and  $(2\times 1)$ -H terminated Si(100) surfaces, as well as for the saturation coverages of six different organic molecules. The third and fourth columns display the Si  $2p$  surface core-level shifts with respect to the Si bulk, and to a hypothetical unbuckled Si(100) surface (SCLS and SCLS $^\dagger$ ; see the text), and the sixth the C  $1s$  shift relative to 284.20 eV (C  $1s$  bulk). The last column lists the experimentally determined saturation coverages in units of molecules per Si-Si dimer.

Adsorbate	Si $2p_{3/2}$ [eV]	SCLS (meV)	SCLS $^\dagger$ (meV)	C $1s$ (eV)	CLS (meV)	$\Theta_{sat.}$
none	98.712/99.262	-488/62	-275/+275	-	-	-
H $_2$	99.473	273	486	-	-	-
C $_2$ H $_2$	99.427	227	440	283.98	-220	0.87
C $_2$ H $_4$	99.031	-169	44	284.21	10	0.84
C $_3$ H $_4$	99.503	303	516	284.49/284.90	290/700	1.15
C $_4$ H $_6$	99.527	327	540	284.45	250	0.79
C $_6$ D $_6$	99.515	315	528	284.52	320	0.36
C $_2$ H $_2$ Cl $_2$	99.496	296	509	283.94/285.42	-260/1220	0.44

is certainly too simple,<sup>11</sup> but should be better than any other choice. Therefore, in Table I, in addition to the difference to the bulk value (SCLS), we also show the difference from this mean value (SCLS $^\dagger$ ). The different reference point results simply in a constant offset (-213 meV) of the SCLS.

Adsorption of hydrogen does lift the up-down asymmetry of the dimers and the charge redistribution connected to it, as corroborated by the single SCLS component found here. Its shift relative to the mean of the clean surface atoms, SCLS of +486 meV, is very large and positive. This might be counterintuitive, since it is contrary to what would be expected from the assumption that hydrogen-terminated Si should be similar to bulk Si because of the small electronegativity difference between Si and H. The binding energy should then be close to the bulk value, not 273 meV higher as found. However, this can be understood by realizing that H atoms contribute much less screening charge to a hole on Si than the bulk Si surrounding. We believe that this is the main reason for the increase relative to the bulk. There may

also be an influence of the dimer geometry which is different from the bulk geometry. This is suggested by the fact that on Si(111)-(1 $\times$ 1)-H—which does not contain dimers—the SCLS is smaller by approximately 80 meV.<sup>37</sup> In comparison with the clean surface, H atoms also remove the occupied and unoccupied surface states (dangling-bond states) which are located close to the Fermi energy and contribute to the additional screening for the clean surface. This supports the view that the SCLS for Si(100)-(2 $\times$ 1)-H relative to the mean of the clean surface atoms, +486 meV, is largely due to the final-state screening. Such strong screening effects, shifts of up to 500 meV, have been calculated for the clean Si(100) surface.<sup>11</sup>

Looking at the sequence of the Si  $2p$  binding energies of the various adsorbates, it becomes obvious that most systems—including hydrogen, but excluding ethylene which will be discussed separately—are quite similar: the SCLS's relative to the mean clean surface value are between 440 and 540 meV. Also, most values (with the exception of acetylene) are more positive than that for hydrogen, although one would expect that the larger molecules contribute more screening charge. Besides different screenings, we expect variations of the chemical shifts; however, in view of the similar electronegativities of C, H, and Si (Pauling electronegativities of 2.55, 2.20, and 1.90, respectively,<sup>38</sup>) these should be small.

There is the striking exception of ethylene, for which a much lower value is found. This is clearest relative to acetylene, which differs only by two H atoms: the difference is almost 400 meV. The sign suggests that there is an additional screening effect for the case of ethylene. Indeed there is an important structural difference between the saturated layers of ethylene and the other hydrocarbons. For the former, the existence of a one-dimensional electronic band structure has been shown,<sup>39</sup> which might also contribute to an enhanced screening, because it eases lateral charge redistribution.

As we have discussed above, the adsorbate C  $1s$  binding energies have no simple correlation to the gas phase binding energies. Therefore the Si-C bonding to the surface seems to play an important role. A comparison of the sequence of the

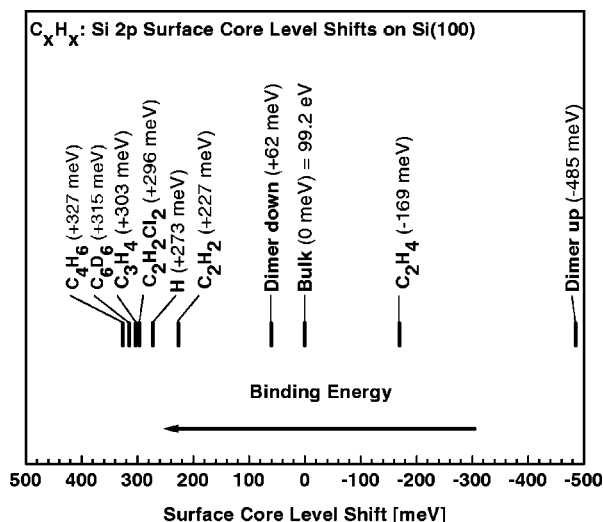


FIG. 6. Surface core-level shifts derived from data shown in Figs. 2, 3, and 4 for different hydrocarbon adsorbates on Si(100)-(2 $\times$ 1). The Si  $2p_{3/2}$  core-level bulk value is set to zero.

C  $1s$  and Si  $2p$  core-level shifts might indicate similar or opposite trends. As a first attempt of a comparison of Si  $2p$  and C  $1s$  shifts, one could assume that adsorbate-induced relaxation shifts should go in the same direction for both core levels, while chemical shifts might go in either direction. Thus a reordering of the sequences should indicate chemical differences. For the C  $1s$  shifts we find the sequence (with decreasing binding energy): 1,2-C<sub>2</sub>H<sub>2</sub>Cl<sub>2</sub>, C<sub>3</sub>H<sub>4</sub>, C<sub>6</sub>H<sub>6</sub>, C<sub>3</sub>H<sub>4</sub>, C<sub>4</sub>H<sub>6</sub>, C<sub>2</sub>H<sub>4</sub>, C<sub>2</sub>H<sub>2</sub>, and 1,2-C<sub>2</sub>H<sub>2</sub>Cl<sub>2</sub> (see Fig. 5 and Table I). For the Si  $2p$  shifts the sequence is C<sub>4</sub>H<sub>6</sub>, C<sub>6</sub>D<sub>6</sub>, C<sub>3</sub>H<sub>4</sub>, and 1,2-C<sub>2</sub>H<sub>2</sub>Cl<sub>2</sub>, H, C<sub>2</sub>H<sub>2</sub>, C<sub>2</sub>H<sub>4</sub> (see Fig. 6). The comparison of both sequences shows that a simple systematic behavior cannot be deduced.

In the following we will discuss aspects of individual systems in more detail. The negative Si  $2p$  SCLS for C<sub>2</sub>H<sub>4</sub> was already discussed on the basis of enhanced screening due to the known one-dimensional band structure. However, this enhanced screening seems to be much weaker for the C  $1s$  hole, since the lowest C  $1s$  energies are found for C<sub>2</sub>H<sub>2</sub> and not for ethylene (+10 versus -220 meV for C<sub>2</sub>H<sub>4</sub> and C<sub>2</sub>H<sub>2</sub>, respectively), which is the reverse sequence to that expected from the gas-phase data. Note that differences in the electronegativities of C<sub>2</sub>H<sub>4</sub> and C<sub>2</sub>H<sub>2</sub> are too small to account for an additional chemical shift.

In the 1,2-C<sub>2</sub>H<sub>2</sub>Cl<sub>2</sub> molecule one hydrogen atom of each carbon atom is substituted with a chlorine atom which has a much larger electronegativity. Assuming for the moment that 1,2-C<sub>2</sub>H<sub>2</sub>Cl<sub>2</sub> adsorbs via di- $\sigma$  bond formation to a Si-Si dimer as in the case of C<sub>2</sub>H<sub>4</sub>, the chlorine atom polarizes the C-Cl bond reducing the charge density at the carbon atom. Thus the available screening charge at the carbon atom is reduced in the 1,2-C<sub>2</sub>H<sub>2</sub>Cl<sub>2</sub> molecule compared to C<sub>2</sub>H<sub>4</sub>, and therefore screening may be less effective in the case of 1,2-C<sub>2</sub>H<sub>2</sub>Cl<sub>2</sub>. This, as well as strong modifications of the initial state, explains the large C  $1s$  shift of 1.22 eV which is expected for carbon bonded to a chlorine atom. For 1,2-C<sub>2</sub>H<sub>2</sub>Cl<sub>2</sub> a Si  $2p$  SCLS of +296 meV in the opposite direction than that for C<sub>2</sub>H<sub>4</sub> is observed. If the available screening charge is dragged away from the carbon by the chlorine in the 1,2-C<sub>2</sub>H<sub>2</sub>Cl<sub>2</sub> molecule, this is also true in second order for the silicon atom of the dimer. The observed sequence of the Si  $2p$  core-level shifts for C<sub>2</sub>H<sub>4</sub> and 1,2-C<sub>2</sub>H<sub>2</sub>Cl<sub>2</sub> is compatible with this model. However, the appearance of a weak second C  $1s$  peak and the possibility of a second Si  $2p$  surface component indicate a more complicated adsorption for 1,2-C<sub>2</sub>H<sub>2</sub>Cl<sub>2</sub> than for C<sub>2</sub>H<sub>2</sub>.

The difference in the Si  $2p$  and C  $1s$  core levels of C<sub>2</sub>H<sub>2</sub> and C<sub>3</sub>H<sub>4</sub> is astonishing since these two molecules are very similar. In the case of C<sub>3</sub>H<sub>4</sub> just one hydrogen atom of C<sub>2</sub>H<sub>2</sub> is substituted for by a CH<sub>3</sub> group. An argument that the polarizability of the additional CH<sub>3</sub> group adds to the screening goes in the opposite direction from what is observed experimentally, since the Si  $2p$  and C  $1s$  shifts are higher for

C<sub>3</sub>H<sub>4</sub>. If one alternatively assumes a different C to Si charge transfer for the adsorbate systems in the initial state, shifts of opposite sign are expected for Si  $2p$  and C  $1s$ . This is again not observed.

Another important difference of the various hydrocarbon adsorbates is the role of the  $\pi$  bonds. While C<sub>2</sub>H<sub>4</sub> is totally saturated after adsorption (no  $\pi$  bonds are left), there is one remaining  $\pi$  bond in C<sub>2</sub>H<sub>2</sub>, C<sub>3</sub>H<sub>4</sub>, and C<sub>4</sub>H<sub>6</sub> and there are two remaining  $\pi$  bonds in C<sub>6</sub>H<sub>6</sub>. However, comparing the polarizabilities of organic molecules in the gas phase, one finds only a small additional polarizability due to the  $\pi$  bonds; e.g., C<sub>2</sub>H<sub>4</sub> and C<sub>2</sub>H<sub>6</sub> have polarizabilities of 4.2 and 4.5 Å<sup>3</sup>, and C<sub>6</sub>H<sub>6</sub> and C<sub>6</sub>H<sub>12</sub> exhibit values of 10.4 and 11.0 Å<sup>3</sup>.<sup>40</sup> Instead, the polarizability scales approximately with the number of C and H atoms. One would predict the sequence C<sub>2</sub>H<sub>2</sub>, C<sub>2</sub>H<sub>4</sub>, C<sub>3</sub>H<sub>4</sub>, C<sub>4</sub>H<sub>6</sub>, C<sub>6</sub>H<sub>6</sub> for increasing core-level shifts. However this model does not fit to the observed core-level shifts to either the Si  $2p$  SCLS's or to the C  $1s$  core-level shifts. Clearly, simple rules,<sup>7</sup> stating that unsaturated bonds typically have binding energies higher by 0.7–0.8 eV than their saturated counterparts or that carbon atoms bonded directly to silicon have binding energies 0.7–0.8 eV lower in energy, do *not* hold for the hydrocarbon adsorbates discussed here.

#### IV. SUMMARY

In the present work we have investigated the core ionization spectra in the region of the C  $1s$  and the Si  $2p$  core levels for six different hydrocarbon molecules on a vicinal single-domain Si(100)-(2×1) surface. From high-resolution XPS data the C  $1s$  core level shift, and the Si  $2p$  surface core level shift, as well as the absolute saturation coverages, have been determined for C<sub>2</sub>H<sub>2</sub>, C<sub>2</sub>H<sub>4</sub>, C<sub>3</sub>H<sub>4</sub>, C<sub>4</sub>H<sub>6</sub>, C<sub>6</sub>H<sub>6</sub>, 1,2-C<sub>2</sub>H<sub>2</sub>Cl<sub>2</sub>, and H, respectively. For the core-level shifts it is not possible to explain the observed sequence with simple models on the basis of domination of either initial- or final-state effects. It seems that the experimentally observed shifts are the results of quite complicated competitions and correlations between the discussed effects. Clearly, theoretical investigations, such as have been successfully applied to the clean Si(100)-(2×1) surface, are needed to understand the details of the core-level shifts. Such an understanding could in turn lead to an improved description of the energetics and dynamics of charge redistribution by bonding and excitation of these species.

#### ACKNOWLEDGMENTS

We thank the staff of ELETTRA, in particular M. Barnaba, for their help at the SuperESCA beamline at ELETTRA, Trieste. This work was supported by the European Community (Project ERBFMGECT950022) and the German BMBF (Grant No. 05SF8WOA).

\*Email address: widdra@e20.physik.tu-muenchen.de, Fax: +49-89-289-12338.

†Present address: II. Institut für Experimentalphysik, Universität Hamburg, 22761 Hamburg, Germany.

<sup>1</sup>J. C. Bean, *High-Speed Superconductor Devices* (Wiley, New York, 1988).

<sup>2</sup>G. Pensl and R. Helbig (unpublished).

<sup>3</sup>C. J. Mogab and H. J. Learnay, *J. Appl. Phys.* **45**(3), 1075 (1974).



- <sup>4</sup>T. Takaoka, T. Takagaki, Y. Igari, and I. Kusunoki, *Surf. Sci.* **347**, 105 (1996).
- <sup>5</sup>I. H. Khan and R. N. Summergrad, *Appl. Phys. Lett.* **11**, 12 (1967).
- <sup>6</sup>G. Dufour, F. Rochet, F. C. Stedile, C. Poncey, M. D. Crescenzi, R. Gunnella, and M. Froment, *Phys. Rev. B* **56**, 4266 (1997).
- <sup>7</sup>H. Liu and R. J. Hamers, *Surf. Sci.* **416**, 354 (1998).
- <sup>8</sup>F. Rochet, F. Jolly, F. Boumel, G. Dufour, F. Sirotti, and J. L. Cantin, *Phys. Rev. B* **58**, 11 029 (1998).
- <sup>9</sup>E. Landemark, C. J. Karlson, Y.-C. Chao, and R. I. G. Uhrberg, *Phys. Rev. Lett.* **69**, 1588 (1992).
- <sup>10</sup>C. Grupp and A. Taleb-Ibrahimi, *J. Electron Spectrosc. Relat. Phenom.* **101-103**, 309 (1999).
- <sup>11</sup>E. Pehlke and M. Scheffler, *Phys. Rev. Lett.* **71**, 2338 (1993).
- <sup>12</sup>T. W. Pi, C. P. Cheng, and I. H. Hong, *Surf. Sci.* **418**, 113 (1999).
- <sup>13</sup>P. Baumgärtel *et al.*, *New J. Phys.* **1**, 1 (1999).
- <sup>14</sup>R. Terborg, P. Baumgärtel, R. Lindsay, O. Schaff, T. Gießel, J. T. Hoefl, M. Polcik, R. L. Toomes, S. Kulkarni, A. M. Bradshaw, and D. P. Woodruff, *Phys. Rev. B* **61**, 16 697 (2000).
- <sup>15</sup>S. Gokhale, A. Fink, P. Trischberger, K. Eberle, and W. Widdra, *J. Vac. Sci. Technol. A* **19**, 706 (2001).
- <sup>16</sup>Sincrotrone Trieste, *ELETTRA Laboratory Beamline Handbook* (Publisher, City, 1996), pp. 1–9.
- <sup>17</sup>S. H. Xu, Y. Yang, M. Keeffe, G. J. Lapeyre, and E. Rotenberg, *Phys. Rev. B* **60**, 11 586 (1999).
- <sup>18</sup>F. C. Stedile, F. Rochet, C. Poncey, G. Dufour, R. Gunella, M. D. Crescenzi, and M. Froment, *Nucl. Instrum. Methods Phys. Res. B* **136-138**, 301 (1998).
- <sup>19</sup>W. Widdra, S. I. Yi, C. Huang, and W. H. Weinberg, *J. Chem. Phys.* **105**, 5605 (1996).
- <sup>20</sup>J. Yoshinobu, H. Tsuda, M. Onchi, and M. Nishijima, *J. Chem. Phys.* **87**, 7332 (1987).
- <sup>21</sup>R. Konečný and D. J. Doren, *Surf. Sci.* **417**, 169 (1998).
- <sup>22</sup>P. A. Taylor, R. M. Wallace, C.-C. Cheng, M. J. Dresser, W. J. Joyke, W. H. Weinberg, and J. T. Yates, Jr., *J. Am. Chem. Soc.* **114**, 6754 (1992).
- <sup>23</sup>C. Huang, W. Widdra, X. S. Wang, and W. H. Weinberg, *J. Vac. Sci. Technol.* **11**, 2250 (1993).
- <sup>24</sup>M. Nishijima, J. Yoshinobu, H. Tsuda, and M. Onchi, *Surf. Sci.* **192**, 383 (1987).
- <sup>25</sup>A. Fink, P. Trischberger, D. Menzel, and W. Widdra (unpublished).
- <sup>26</sup>A. Fink, Ph.D. thesis, Technische Universität München, 2001.
- <sup>27</sup>P. Baumgärtel, J. J. Paggel, M. Hasselblatt, K. Horn, V. Fernandez, O. Schaff, J. H. Weaver, A. M. Bradshaw, D. P. Woodruff, E. Rotenberg, and J. Denlinger, *Phys. Rev. B* **59**, 13 014 (1999).
- <sup>28</sup>R. I. G. Uhrberg, E. Landemark, and Y.-C. Chao, *J. Electron Spectrosc. Relat. Phenom.* **75**, 197 (1995).
- <sup>29</sup>S. Gokhale, P. Trischberger, H. Dröge, H.-P. Steinrück, U. Gutdeutsch, U. Birkenheuer, N. Rösch, D. Menzel, and W. Widdra, *J. Chem. Phys.* **108**, 5554 (1998).
- <sup>30</sup>A. Pasquarello, M. S. Hybertsen, and R. Car, *J. Vac. Sci. Technol. B* **14**, 2809 (1996).
- <sup>31</sup>N. Mårtensson and A. Nilsson, *J. Electron Spectrosc. Relat. Phenom.* **75**, 209 (1995).
- <sup>32</sup>T. D. Thomas, *J. Chem. Phys.* **52**, 1373 (1970).
- <sup>33</sup>R. McLaren, S. A. C. Clark, I. Ishii, and A. P. Hitchcock, *Phys. Rev. A* **36**, 1683 (1987).
- <sup>34</sup>A. P. Hitchcock, S. Beaulieu, T. Steel, J. Stöhr, and F. Sette, *J. Chem. Phys.* **80**, 3927 (1984).
- <sup>35</sup>J. Stöhr, *NEXAFS Spectroscopy*, Springer Series in Surface Sciences Vol. 25 (Springer, New York, 1992); and (private communication).
- <sup>36</sup>J. J. Pireaux, S. Svensson, E. Basilier, P.-A. Malmquist, U. Gelius, R. Caudano, and K. Siegbahn, *Phys. Rev. A* **14**, 2133 (1976).
- <sup>37</sup>C. J. Karlsson, F. Owman, E. Landemark, Y.-C. Chao, P. Mårtensson, and R. I. G. Uhrberg, *Phys. Rev. Lett.* **72**, 4145 (1994).
- <sup>38</sup>Sargent-Welch, *Periodic Properties of the Elements* (1980).
- <sup>39</sup>W. Widdra, F. Fink, S. Gokhale, P. Trischberger, U. Gutdeutsch, U. Birkenheuer, N. Rösch, and D. Menzel, *Phys. Rev. Lett.* **80**, 4269 (1998).
- <sup>40</sup>A. Radzig and B. Smirnov, *Reference Data on Atoms, Molecules, and Ions*, Chemical Physics Vol. 31 (Springer, New York, 1985).
- <sup>41</sup>G. Remmers, M. Domke, and G. Kaindl, *Phys. Rev. A* **47**, 3085 (1993).
- <sup>42</sup>In the core-level region the resolution is better because for the electron analyzer used it increases with decreasing retarding voltage.
- <sup>43</sup>Note that Ref. 7 used a value of 99.4 eV as the energy standard for the Si  $2p_{3/2}$  bulk core level, while we use 99.2 eV.